SUPPORTING INFORMATION (SI)

APPENDIX

SUPPLEMENTARY MATERIALS & METHOD

Archived clinical patient brain tissue processing & data collection

Frozen, postmortem, human brain tissue containing the DLPFC (Brodman Area 46) was obtained from the Harvard Brain Tissue Resource Center. Because these patients cannot be identified, no IRB approval was required. and permission to use the samples for research was given by the donors at the time they made their anatomical gifts. The demographics of the patients whose donated brains were used is summarized in **Table S1**.

Total protein was extracted, Halt protease and phosphatase inhibitor cocktails (Fisher) were added and total protein concentration was quantified. Samples were separated on 4-20% Mini-Protein TGX gels (Bio-Rad), then transferred to PVDF membranes. Then membranes were blocked and probed with primary antibodies. After incubation with HRP-conjugated secondary antibodies, immunocomplexes were visualized using Western Lightning Plus ECL (Perkin Elmer). Semi-quantitative assessment of protein bands was executed by computerized densitometry using the ChemiDoc XRS+ System (Bio-Rad) and Image Lab Software (Bio-Rad). Chemiluminescent values of the protein bands were divided by its corresponding NSE chemiluminescent values. The SCZ values were normalized to control values (% control) collected in parallel from the same gel.

Tissue Processing

Tissue samples were processed as previously described (1). Briefly, samples were dissected to produce two tissue blocks measuring 1.5 cm2 × 0.5 cm and 1.5 cm2 × 0.2–0.3 cm, respectively. The first block was stained using the Golgi-Kopsch method. Tissue blocks were shaken in a 4% potassium dichromate in 5% paraformaldehyde solution at room temperature in the dark for 96 hours. The potassium dichromate/paraformaldehyde solution was replaced every 36 hours and acid-cleaned glassware was utilized. Tissue blocks were washed in increasing concentrations of silver nitrate (0.25, 0.5, 0.75 and 1%) and then shaken in 1% silver nitrate in acid-cleaned glassware at room temperature in the dark for 1 week. Stained tissue blocks were sectioned using a vibrating microtome (Vibratome, St. Louis, MO) at 100 μm, mounted on gelatin-coated slides, and briefly air-dried. Tissue sections were then dehydrated with a graded series of ethanol, cleared with xylene and cover-slipped with Permount (Fisher Scientific). The second block was sectioned using a vibrating microtome at 40 μm, mounted on gelatin-coated slides, and air-dried. The tissue sections were then stained for cytoplasmic ribonucleic acid (Nissl substance) using thionin and cover-slipped.

Pyramidal Cell Reconstruction

Procedures were identical to those previously described (1, 2). All analyses were conducted by a single investigator (G.T.K.) blinded to subject number and diagnosis. Nissl-stained sections were used to confirm

localization to DLPFC using established cytoarchitectonic criteria and to ascertain the borders of layer III as a percentage of cortical thickness. Fifteen Golgi-stained pyramidal cells were selected for reconstruction per subject using the following criteria (3): (a) somata located in the bottom half of layer III and in the middle of the section thickness; (b) pyramidal cell fully impregnated; (c) somata or dendrites not obscured by large (>5 μm) staining opacities; (d) no morphological changes associated with postmortem interval; and (e) presence of ≥3 basilar dendrites each branching at least once. For each selected pyramidal cell, the apparently longest basilar dendrite was selected visually and reconstructed using Neurolucida (version 11, MicroBrightfield Bioscience, Williston, VT) with a Zeiss Axioskop 2 Plus light microscope (Carl Zeiss, Germany) and a ×100 oil immersion objective (NA=1.4, working distance=0.17 mm). Reconstructions were done on live images captured using an CX9000 digital camera (MicroBrightfield Bioscience, Williston, VT) at a final resolution of 1600 × 1200. Each dendrite terminus was classified as ending naturally or artificially at the cut surface of the section.

Statistical analyses of data from clinical human postmortem brain tissue

All statistical analyses for data from human patient postmortem brain tissue were conducted using STATA (v. 12, College Station, TX). As stated above, normalized relative protein expression values were used. Inter-group protein expression differences were assessed using an ANCOVA model. Covariates were selected from age, sex, postmortem interval (PMI), storage time, and pH using Aikake's Information Criterion corrected for small samples (AICc).

Correlation with dendrite parameters

For each differentially-expressed protein or ratio, the relationship between its value and basilar dendrite parameters for pyramidal cells in the deep half of layer III in the DLPFC was assessed. A Pearson correlation coefficient was calculated for the relative protein expression level or ratio and the number of spines per basilar dendrite, basilar spine density, and basilar dendrite length.

Patients from whom PBMCs were collected

The demographics of the SCZ and healthy control patients (ranging in age from 18-40 years old) from whom PBMCs were collected are summarized in **Table S2.** Such data includes age and sex, family medical history, smoking history, drinking history, education, career, medication history. They were inpatients or outpatients at Yokohama City University Hospital, Yokohama Medical Center, or Yokohama Maioka Hospital (affiliated with Yokohama City University). The study was approved by the Ethical Review Board of each hospital. Each SCZ patient was diagnosed by at least two psychiatrists based on the diagnostic criteria of Diagnostic & Statistical Manual of Mental Disorders (DSM-IV). The PANSS (Positive and Negative Symptom Scale) was used to assess symptom severity. For matched unaffected controls, volunteers were

enlisted by a general open call. Each volunteer was interviewed by psychiatrists to exclude mental disorders. Informed consent was obtained from all participants. Samples were assessed blindly by the investigators.

Blood sample collection and lymphocyte separation

PBMCs were isolated from all collected blood samples using a mononuclear cell preparation tube (BD Vacutainer CPT:Becton–Dickinson, NJ,USA). The whole blood specimens were centrifuged for 30 min (1500g, 25℃) to collect a PBMC layer in 15-ml tubes. These samples were then washed with phosphate-buffered saline minus (PBS) and centrifuged three times at 427 g for 10 min at 4℃. After discarding the supernatant, the pellet was resuspended in RPMI1640 medium supplemented with 10% fetal bovine serum (FBS) and ampicillin. The resuspended samples were plated on the non-coated Petri dish and left in CO_2 incubator at 37℃ for two days. The supernatant fraction containing non-adherent lymphocytes was collected and transferred to 15-ml tubes. The samples were centrifuged at 200 g for 5 min at 4℃. After discarding the supernatants, the pellets were resuspended in 1 ml PBS, and transferred to 1.5 ml tubes. After centrifuging at 200 g for 5 min at 4℃, the supernatants were discarded and the pellets were frozen with liquid nitrogen and stored at -80℃ until use. CRMP2 and p-CRMP2 levels were subsequently assessed in these samples as described below

Antibodies

An anti-human CRMP2 monoclonal antibody (9F) was raised by injection of a C-terminal region of human CRMP2 (amino acid 486-528) into Balb/c mice (18). An anti-phosphorylated CRMP1/2(S522) (p-S522-CRMP1/2) polyclonal antibody that recognizes CRMP2 phosphorylated at Ser522 was generated as previously described in rabbits (4). The specificities of the two antibodies were verified by peptide-blocking experiment in immunoblot analysis of human PMBC samples as previously described (4-6). (See **Figs. S2 & S3**). Immunoblots of wild-type and CRMP2-KO mouse brains were used to confirm the specificity of the anti-CRMP2 antibodies. The use of these animals for this purpose was approved by the institutional Animal Care and Use Committee (IACUC) of the Yokohama City University Graduate School of Medicine.

Immunoblot analysis

Sample pellets were homogenized in 50 μl immunoprecipitation IP buffer (20 mM Tris-HCL, pH 8.0, 150 mM NaCl, 1 mM EDTA, 10 mM NaF, 1 mM Na_3VO_4, 1 % Nonidet P-40, 50 μM ρ-APMSF［ρ-amidinophenylmethanesulfonyl fluoride］), and were centrifuged at 15 000g for 20 min at 4℃. The samples were then used for immunoblot analysis with anti-CRMP2 (9F), anti-phosphorylated CRMP1/2, and anti-β-actin mouse monoclonal (A5316, Sigma-Aldrich, MO, USA) antibodies with signal enhancer HIKARI (Nacalai Tesque, Kyoto, Japan). Actin (2.0 mg/ml) and rat brain lysate (0.5 mg/ml) were used as loading controls. Purified CRMP2 was used as a standard to calculate concentration of CRMP2 in lymphocyte lysate

in immunoblotting by using ImageJ. The relative amounts of CRMP2 and its Ser522 phosphorylated form of CRMP2 (p-S522-CRMP2) were estimated using β-actin as an internal standard. (See **Figs. S2 & S3**)

Statistical analysis of data from peripheral blood specimens

Statistical analysis was conducted using IBM SPSS Statistics 22 (IMB Analysis). For a Mann-Whitney U test, statistical significance was considered to be $p < 0.05$. For examination between continuous variables, a regression analysis was conducted; significance of the correlation coefficient was considered to be $p < 0.05$.

SUPPLEMENTARY TABLES

TABLE S1: Demographic information on patients whose postmortem brains were analyzed

TABLE S1

Demographic information on patients whose brains were analyzed

	Schizophrenia	Control	*p*-value
Sex (M/F)	13/6	14/5	
Age	59.5±12.7	55.8±12.3	*n.s.*
Postmortem interval (hours)	23.9±6.6	22.5±3.9	*n.s.*
Storage time (months)	137.3±30.5	119.7±18.6	*n.s.*
pH	6.5±0.3	6.4±0.2	*n.s.*

TABLE S2: Demographic information on patients whose PBMCs were analyzed

TABLE S2

Demographic information on patients whose PBMCs were analyzed

	Control Subjects (Total)	Control Subjects (≦30 years old)	Control Subjects (30<,≦40)
N	37	25	12
Sex	M : 19 F : 18	M : 12 F : 13	M : 7 F : 5
Age (years)	29.1	25.5	36.7
Education (years)	19.3	17.6	20.3

	Schizophrenia Patients (Total)	Schizophrenia Patients (≦30 years old)	Schizophrenia Patients (30<,≦40)
N	21	13	8
Sex	M : 9 F : 12	M : 4 F : 9	M : 5 F : 3
Age (years)	28.5	23.7	36.4
Disease period (years)	8.4	4.0	15.6
Quantity of medication (CP conversion:mg)	668.3	834.2	398.6
GAF[※1]	44.7	40.5	52.4
PANSS[※2]			
Positive subscale score	19.4	20.2	16.8
Negative subscale score	21.6	22.7	18.0
General psychopathology score	44.2	46.1	37.8
Total score	84.6	89.0	70.0
Education (years)	14.1	13.9	14.4

※1 GAF : The Global Assessment of Functioning

※2 PANSS : Positive and Negative Syndrome Scale

SUPPLEMENTARY FIGURES

FIGURE S1:

Although CRMP2 levels were significantly higher in brains from SCZ patients compared to those from unaffected controls (as per *Fig. 1C*), the p-CRMP2 protein expression in those SCZ brains *[A]* and, hence, the ratio of p-CRMP2 : CRMP2 protein expression *[B]* initially appeared not to be significantly different from controls ($p > 0.05$) when the cohorts were examined in the *aggregate*. These findings suggested the following possibilities: **(i)** in the brain, the process of phosphorylating (and, hence, inactivating) the increased CRMP2 substrate could keep pace with the greater burden; or **(ii)** that p-CRMP2 was rising for reasons independent of SCZ (because of the stochastic, serendipitous nature of brain banking for psychiatric disorders, this cohort was older than the one whose PBMCs were subsequently examined – compare **Table S1** with **Table S2**), and p-CRMP2 often rises in association with aging-related conditions; or **(iii)** lymphocytes are more sensitive than the brain for showing alterations in the ratio (perhaps because they are shorter-lived).

Of note was an informative finding that emerged from focusing only on the few patients <40 years of age (those indicated in **Fig. 1**). Among the unaffected controls, the brain indicated by the **pink arrow** and **green dot** came from a 36 year old female with CRMP2 levels of 82.2 (within normal limits, 98% of mean control) and a p-CRMP2 level of 107.2 (also within normal limits). Among the SCZ patients, the brain indicated by the **blue arrow** and **green square** came from a 23 year-old female with a *CRMP2* level *elevated to 129.7* (162% of control, as per **Fig. 1C**) but a with a p-CRMP2 level within normal limits (104.5, which is 97.2% of control). While the p-CRMP2:CRMP2 ratio in the unaffected control brain was 1.3 (within normal limits), the ratio in the SCZ brain was *quite abnormally low* at 0.8 (~40% lower).

As is seen in **Fig. 2**, when the cohort is limited to young, new-onset, newly-presenting, and/or newly-diagnosed SCZ patients (i.e., patients <40 years-of-age), not only does *active CRMP2 increase*, but p-CRMP2 remains stably normal, hence *decreasing* the *pCRMP2 : CRMP2 ratio* (in contrast to that seen in unaffected controls and dramatically different from that seen in LiR BPD patients (2, 7)).

To obtain the data presented here, quantitative Western Blots were performed. Absolute values of the *CRMP2* and *p-CRMP2* protein levels were obtained by normalizing the chemiluminescent values of their respective protein bands to corresponding neuron specific enolase (NSE) chemiluminescence as an internal standard and then giving them arbitrary units based on that normalization. The SCZ values were further normalized to control values (% control) collected in parallel from the same gel.

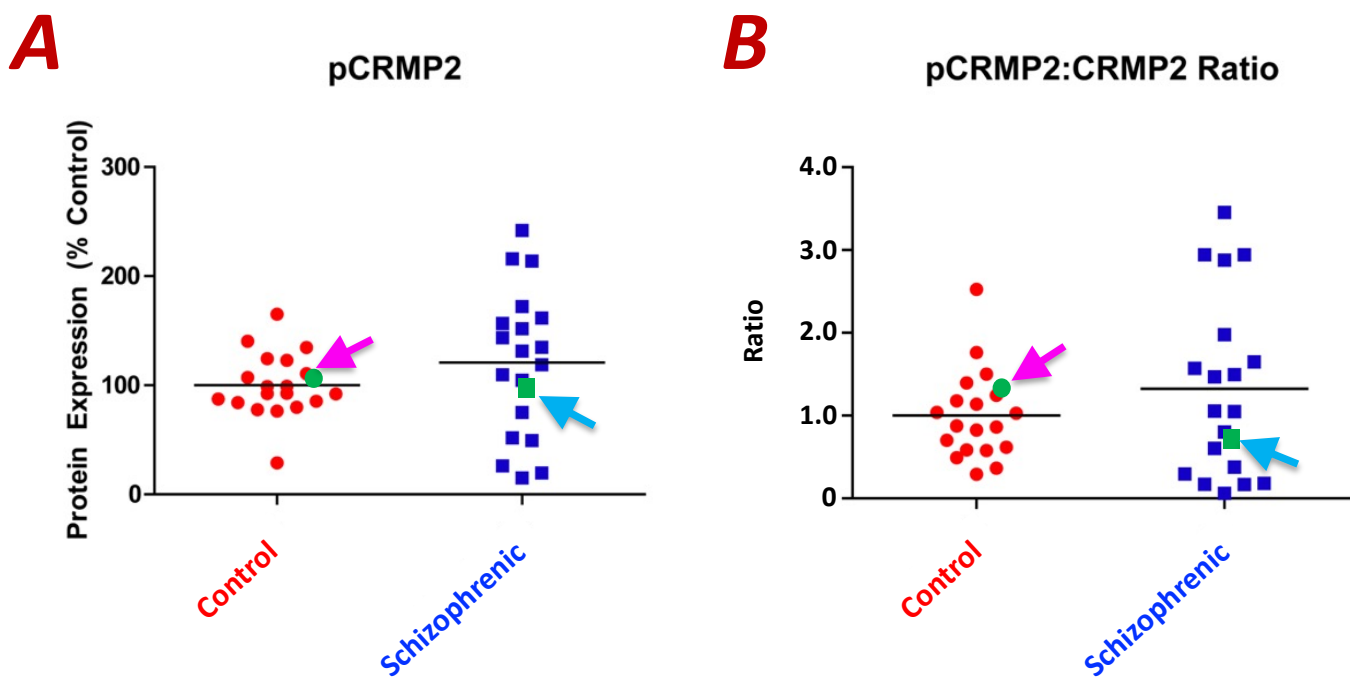
A
pCRMP2
Protein Expression (% Control)
300
200
100
0
Control
Schizophrenic
B
pCRMP2:CRMP2 Ratio
Ratio
4.0
3.0
2.0
1.0
0
Control
Schizophrenic

Figure S1

FIGURE S2:

Authentication of the sensitivity and specificity of the antibodies against CRMP2 and the phosphorylated form of CRMP2 based on immunoblot analysis.

[A] Specificity of the anti-CRMP2 monoclonal antibody (9F) **[Upper Panel]** and the anti-phosphorylated CRMP1/2(S522) (pS522-CRMP2) polyclonal antibody **[Lower Panel]** demonstrated by immunoblot analysis of the brain lysates from *wild type* (*wt*), *crmp1*$^{-/-}$, *crmp2*$^{-/-}$, *crmp1*$^{-/-}$;*crmp2*$^{-/-}$ and CRMP2S522A knock-in (*crmp2*$^{ki/ki}$) mice. In the **Upper Panel**, a single band of 64 kDa was detected with 9F in brain lysates from *wt*, *crmp1*$^{-/-}$ and *crmp2*$^{ki/ki}$ mice, but was missing in *crmp2*$^{-/-}$ mice. In the **Lower Panel**, a single band was detected with anti-pS522-CRMP2 antibody in brain lysates from *wt* and *crmp1*$^{-/-}$, but not in *crmp1*$^{-/-}$;*crmp2*$^{-/-}$ and *crmp2*$^{ki/ki}$ mice.

[B] A representative immunoblot with anti-CRMP2 antibodies directed against human peripheral blood mononuclear cell (PBMC) fractions from normal healthy control subjects **[Left Panel]** compared to positive control brain lysates. In the **Right Panel**, the bands are seen to be successfully blocked by antigen peptide of CRMP2. (See also **Figure S3** for further validation of the antibodies used in this study)

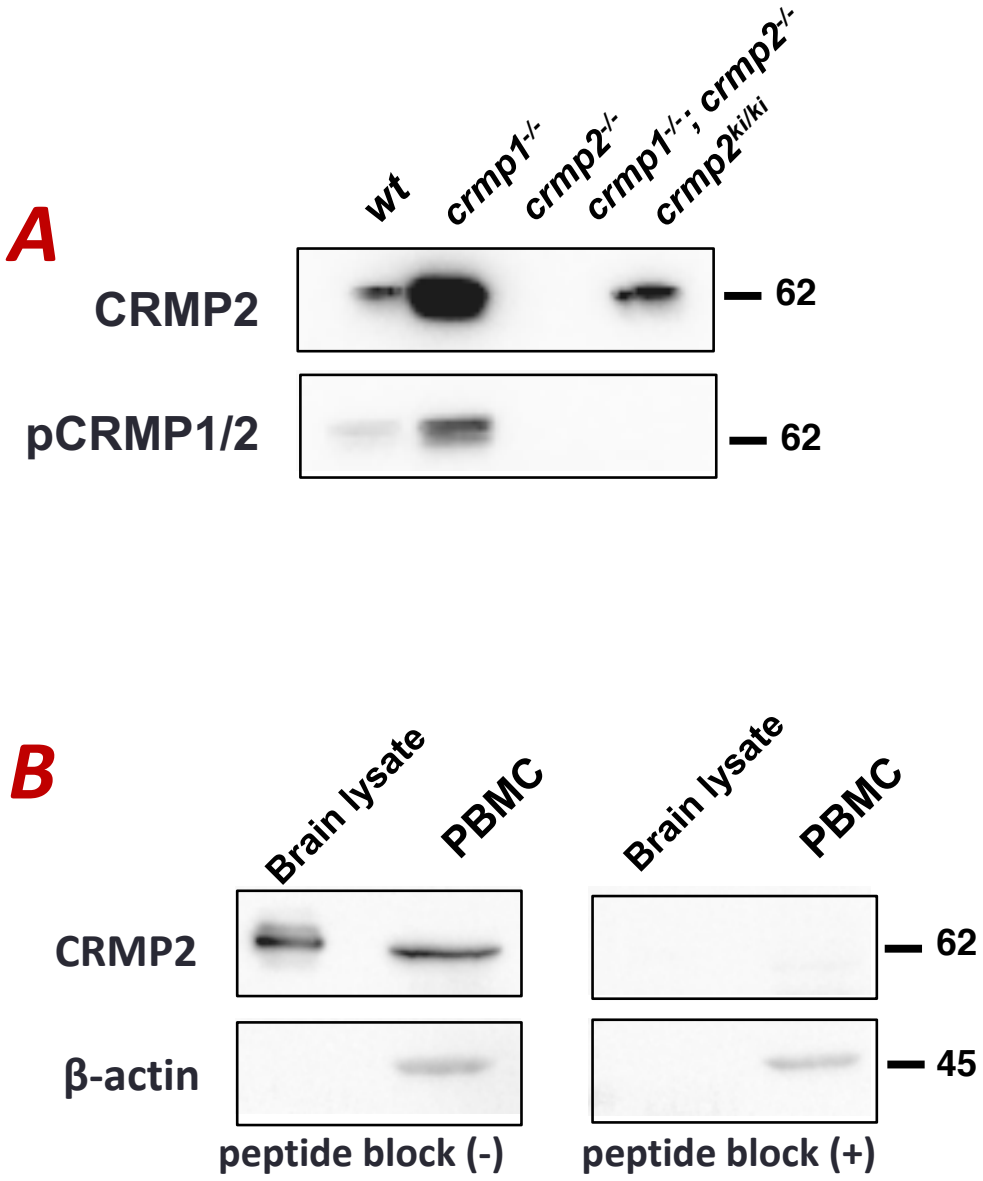
A
wt
crmp1-/-
crmp2-/-
crmp1-/-; crmp2-/-
crmp2ki/ki
CRMP2
62
pCRMP1/2
62
B
Brain lysate
PBMC
Brain lysate
PBMC
CRMP2
62
β-actin
45
peptide block (-)
peptide block (+)

Figure S2

FIGURE S3:

Further validation of antibodies used for immunoblotting in this study and evidence that the CRMP*1* isoform is not pertinent to the phenomena described in this study. That the differences seen in SCZ vs. unaffected patients pivoted on differences in the abundance of the CRMP*2* isoform rather than of the CRMP*1* isoform was proven through the use of antibodies against CRMP*1*, as well; none of the differences described in this study were related to CRMP*1*. This figure shows immunoblot analysis using 2 different anti-CRMP1 antibodies (2E7G and 2C6G) against wild (*WT*) and *crmp1*$^{-/-}$ (CRMP1 KO) or *crmp2*$^{-/-}$ (CRMP2 KO) mouse brain lysates, as well as human peripheral blood mononuclear cell (PBMC) fractions (specifically, lymphocytes). In brain lysates from *wt* mice, a single band was detected by 2E7G and 2C6G, but not in the brain lysates from CRMP1-knockout mice, thereby showing the specificity of these anti-CRMP1 antibodies. In this analysis, using these 2 sensitive CRMP1 antibodies, CRMP1 was not detected in human lymphocyte samples (**a, b**).

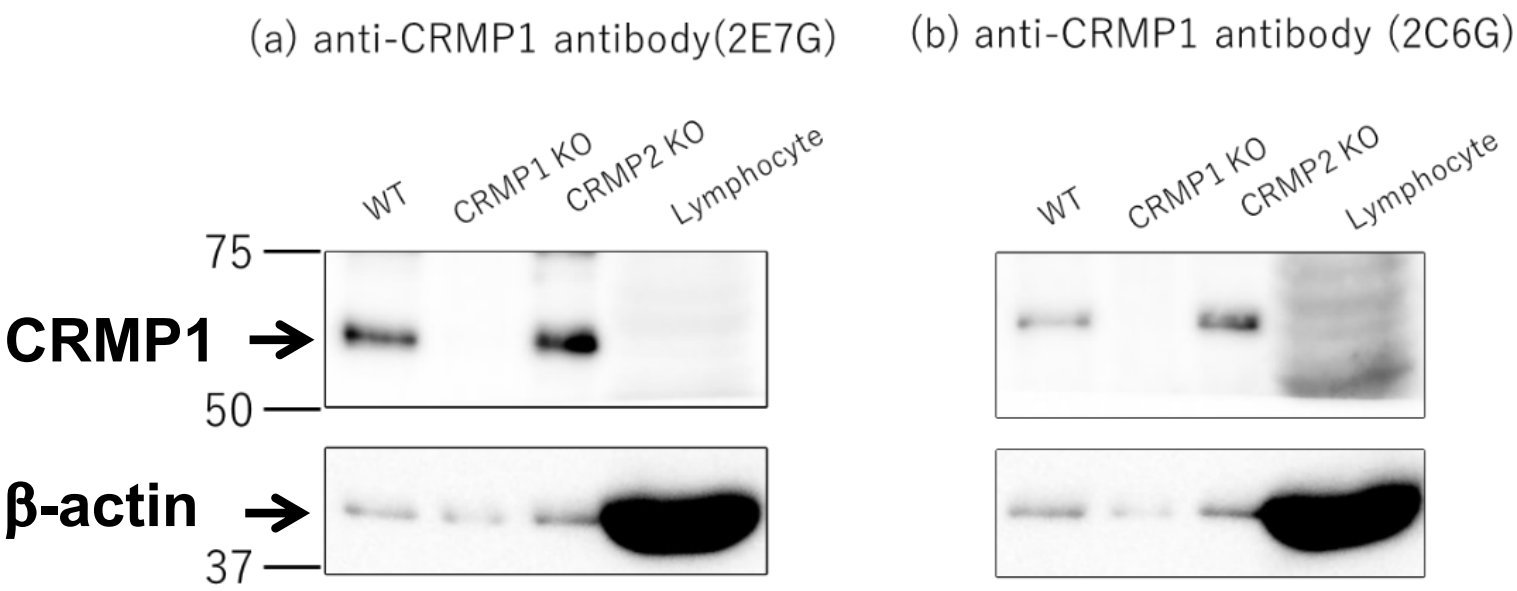
(a) anti-CRMP1 antibody(2E7G)
WT
CRMP1 KO
CRMP2 KO
Lymphocyte
75
CRMP1
50
β-actin
37
(b) anti-CRMP1 antibody (2C6G)
WT
CRMP1 KO
CRMP2 KO
Lymphocyte

Figure S3

SUPPLEMENTAL INFORMATION (SI) REFERENCES

1. Konopaske GT, et al (2014), Prefrontal cortical dendritic spine pathology in schizophrenia and bipolar disorder, *JAMA Psych* 71(12): 1321-31.
2. Tobe BTD, *et al*. (2017) Probing the lithium-response pathway in hiPSCs implicates the phosphoregulatory set-point for a cytoskeletal modulator in bipolar pathogenesis. *Proc Natl Acad Sci USA*. 114 (22), E4462-E4471.
3. Glantz LA, Lewis DA (2000) Decreased dendritic spine density on prefrontal cortical pyramidal neurons in schizophrenia. *Arch Gen Psych*. 57(1): p. 65-73.
4. Uchida Y, *et al*. (2005) Semaphorin3A signaling is mediated via sequential Cdk5 and GSK3beta phosphorylation of CRMP2: implication of common phosphorylating mechanism underlying axon guidance and Alzheimer's disease. *Genes Cells* 10(2):165-179.
5. Higurashi M, *et al*. (2012) Localized role of CRMP1 and CRMP2 in neurite outgrowth and growth cone steering. *Develop Neurobiol* 72(12):1528-1540.
6. Makihara H, *et al*. (2016) CRMP1 and CRMP2 have synergistic but distinct roles in dendritic development. *Genes Cells* 21(9):994-1005.
7. Zhao, W., *et al*. (2020) Discovery of suppressors of CRMP2 phosphorylation reveals compounds that mimic the behavioral effects of lithium on amphetamine-induced hyperlocomotion. *Transl Psychiatry* **10,** 76.